

AL-TR-1991-0044

AD-A251 610



ARMSTRONG

## NONINVASIVE MEASUREMENT OF CURRENT FOR DOSIMETRY

Mark J. Hagmann  
Tadeusz M. Bablj

Department of Electrical and Computer Engineering  
Florida International University  
Miami, FL 33199

OCCUPATIONAL AND ENVIRONMENTAL  
HEALTH DIRECTORATE  
Brooks Air Force Base, TX 78235-5000

DTIC  
ELECTE  
JUN 10 1992  
S B D

May 1992

Final Technical Report for Period August 1989 - August 1990

Approved for public release; distribution is unlimited.

92-15087



92 6 08 080

AIR FORCE SYSTEMS COMMAND  
BROOKS AIR FORCE BASE, TEXAS 78235-5000

LABORATORY


## NOTICES

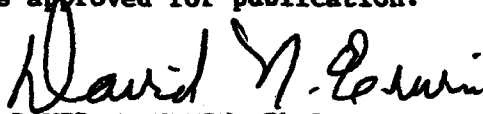
When Government drawings, specifications, or other data are used for any purpose other than in connection with a definitely Government-related procurement, the United States Government incurs no responsibility or any obligation whatsoever. The fact that the Government may have formulated or in any way supplied the said drawings, specifications, or other data, is not to be regarded by implication, or otherwise in any manner construed, as licensing the holder or any other person or corporation; or as conveying any rights or permission to manufacture, use, or sell any patented invention that may in any way be related thereto.


The voluntary, fully informed consent of the subjects used in this research was obtained as required by AFR 169-3.

The Office of Public Affairs has reviewed this report, and it is releasable to the National Technical Information Service, where it will be available to the general public, including foreign nationals.

This report has been reviewed and is approved for publication.

  
WILLIAM D. HURT, M.S.  
Project Scientist

  
DAVID N. ERWIN, Ph.D.  
Chief, Radiofrequency Radiation  
Branch

  
MICHAEL L. BINION, Lt Col, USAF, BSC  
Chief, Directed Energy Division

**REPORT DOCUMENTATION PAGE**Form Approved  
OMB No. 0704-0188

Public reporting burden for this collection of information is estimated to average 1 hour per response, including the time for reviewing instructions, searching existing data sources, gathering and maintaining the data needed, and completing and reviewing the collection of information. Send comments regarding this burden estimate or any other aspect of this collection of information, including suggestions for reducing this burden, to Washington Headquarters Services, Directorate for Information Operations and Reports, 1215 Jefferson Davis Highway, Suite 1204, Arlington, VA 22202-4302, and to the Office of Management and Budget, Paperwork Reduction Project (0704-0188), Washington, DC 20503.

<b>1. AGENCY USE ONLY (Leave blank)</b>		<b>2. REPORT DATE</b> May 1992	<b>3. REPORT TYPE AND DATES COVERED</b> Final - August 1989 - August 1990	
<b>4. TITLE AND SUBTITLE</b> Noninvasive Measurement of Current for Dosimetry			<b>5. FUNDING NUMBERS</b> C - F33615-87-D-0626 PE - 62202F PR - 7757 TA - 01 WU - 2D	
<b>6. AUTHOR(S)</b> Mark J. Hagmann Tadeusz M. Babij				
<b>7. PERFORMING ORGANIZATION NAME(S) AND ADDRESS(ES)</b> Department of Electrical and Computer Engineering Florida International University Miami, FL 33199			<b>8. PERFORMING ORGANIZATION REPORT NUMBER</b>	
<b>9. SPONSORING/MONITORING AGENCY NAME(S) AND ADDRESS(ES)</b> Armstrong Laboratory Occupational and Environmental Health Directorate Brooks Air Force Base, TX 78235-5000			<b>10. SPONSORING/MONITORING AGENCY REPORT NUMBER</b> AL-TR-1991-0044	
<b>11. SUPPLEMENTARY NOTES</b>  Armstrong Laboratory Technical Monitor: William D. Hurt, (512) 536-3185				
<b>12a. DISTRIBUTION/AVAILABILITY STATEMENT</b>  Approved for public release; distribution is unlimited.			<b>12b. DISTRIBUTION CODE</b>	
<b>13. ABSTRACT (Maximum 200 words)</b>  Minimally perturbing, resistive, non-ferrous probes were developed for measuring the current induced in personnel exposed to electromagnetic fields, with particular emphasis on the pulsed fields in electromagnetic pulse (EMP) simulations. Each of these probes has a non-ferromagnetic toroid that passes around the leg or other body member, and a coil formed from high-resistance line that is evenly distributed over the full length of the toroid. A mental electrostatic shield is used to limit capacitive coupling. Active elements were not used in the probe circuitry so the probes have maximum ruggedness for use in high intensity EMP fields. These probes have sufficient bandwidth for time-domain measurements in EMP simulations. The probes are compatible with the low-impedance (50 ohms) fiber-optics transducers typically used for data acquisition in EMP simulations.				
<b>14. SUBJECT TERMS</b> Currents induced in humans Dosimetry Electromagnetic pulse			<b>15. NUMBER OF PAGES</b> 36	
			<b>16. PRICE CODE</b>	
<b>17. SECURITY CLASSIFICATION OF REPORT</b> Unclassified	<b>18. SECURITY CLASSIFICATION OF THIS PAGE</b> Unclassified	<b>19. SECURITY CLASSIFICATION OF ABSTRACT</b> Unclassified	<b>20. LIMITATION OF ABSTRACT</b> UL	

# TABLE OF CONTENTS

	<u>Page</u>
INTRODUCTION. . . . .	1
DESCRIPTION OF OUR EARLIER CURRENT PROBES . . . . .	2
CALIBRATION PROCEDURES. . . . .	5
Standard Shielded Test Fixtures. . . . .	5
New Shielded Test Fixtures . . . . .	5
Loop Test Fixtures . . . . .	6
RFI SUSCEPTIBILITY. . . . .	7
Decreasing RFI Susceptibility of the New Probes. . . . .	7
RFI Susceptibility of Commercial Current Probes. . . . .	8
MODIFICATIONS OF THE CURRENT PROBES . . . . .	8
Electrostatic Shield . . . . .	8
Coil Resistance. . . . .	9
Increasing Bandwidth . . . . .	10
Description of the Completed Probes. . . . .	10
INSERTION IMPEDANCE OF CURRENT PROBES . . . . .	11
ANALYSIS OF CURRENT PROBES. . . . .	13
Commercial Current Probes. . . . .	13
Non-Ferromagnetic Probe with Axial Current . . . . .	13
Non-Ferromagnetic Probe with Off-Axis Current. . . . .	16
Probe Coil/Shield as a Transmission Line . . . . .	20
FIELD TESTING AT THE ALECS FACILITY . . . . .	23
FIELD TESTING AT THE EMPRESS I FACILITY . . . . .	25
SUGGESTIONS FOR FUTURE WORK . . . . .	27
REFERENCES. . . . .	27

Accession For	
NTIS GRA&I	<input checked="" type="checkbox"/>
DTIC TAB	<input type="checkbox"/>
Unannounced	<input type="checkbox"/>
Justification	
By _____	
Distribution/	
Availability Codes	
Dist	Avail and/or Special
A-1	



## List of Figures

### Fig. No.

1. Block Diagram of New Current Probe . . . . .	3
2. Derivation for Ferromagnetic Current Probe . . . .	14
3. Derivation for Non-Ferrous Current Probe . . . . .	15
4. Non-Ferrous Core with an off-Axis Current Filament.	17
5. Transmission Line Model of the Probe Coil Shield. .	21

## List of Tables

### Table No.

I. Measurements of Impedance . . . . .	12
II. Summary of Measurements at the ALECS Facility . . .	24
III. Summary of Measurements at the EMPRESS I Facility .	26

# NONINVASIVE MEASUREMENT OF CURRENT FOR DOSIMETRY

## 1. INTRODUCTION

The project objective was to develop minimally perturbing probes for measuring the current induced in workers exposed to electromagnetic fields (EMF), with particular emphasis on the pulsed fields in electromagnetic pulse (EMP) simulations. The primary significance of this project to the Air Force is that possible hazards, from exposure of personnel to EMF, may be better characterized and understood.

To achieve our objective, it was necessary to make major changes in the design of minimally perturbing current probes which we had developed before this project. The earlier probes were designed for fixed-frequency measurements [1]-[4], so they are loaded by diode detectors, and the rectified output is connected to (high-impedance) readout electronics by resistive line. By contrast, time-domain measurements are required in EMP simulations, so the probe must have a much larger bandwidth, and the time-dependent (unrectified) output of the probe should be compatible with a low-impedance (50 ohms) fiber-optics transducer for data acquisition. Additional circuitry with active components is not recommended because of the high intensity of the EMP fields. Major changes were made in the earlier current probes to obtain greater bandwidth and ruggedness, and to decrease the output impedance, radiofrequency interference (RFI) susceptibility, and sensitivity.

Clamp-on alternating current (AC) ammeters are commonly used to measure electrical current without interrupting a circuit, and high-frequency current probes are used for the same purpose in RF applications as well as in EMP simulations [5],[6]. These commercial instruments use a ferromagnetic core to couple the magnetic flux produced by the current to a coil, and the voltage induced in this coil is measured to evaluate the current (See Section 7). If the current is induced in an object by ambient fields (rather than current driven through a wire by a voltage source), then the commercial instruments would not be appropriate since the ferromagnetic core, wire coil, and metal shield would alter the fields and, hence, change the current.

Gronhaug has made theoretical and experimental studies of the currents induced in personnel exposed to the fields of EMP simulators [7]-[9]. He measured the current in the (horizontal) arms of human volunteers exposed with a horizontally polarized dipole (HPD) simulator [8], and the current in the legs for exposure with a vertically polarized dipole (VPD) simulator [9]. The maximum values of peak current, which were measured in the ankles for VPD exposure, were 4.3 A with bare feet and 2.7 A with the feet insulated by standing on a dry wooden board using rubber-soled shoes [9].

Gronhaug [9] used a commercial current probe having a 10-cm diameter aperture (Ailtech 94456-2), which was the largest size available to him, in all of his measurements. This probe has a ferromagnetic core, a wire coil, and a metal shield, so it would cause significant perturbations to the EMFs. Commercial current probes have also been used by other researchers to measure the current induced in the legs of human subjects under fixed frequency conditions [10].

## 2. DESCRIPTION OF OUR EARLIER CURRENT PROBES

Earlier, we developed minimally perturbing current probes for fixed-frequency measurements [1]-[4]. A block diagram for these devices is shown in Fig. 1. Each of these probes has an air-core toroid that passes around the leg or other body member, and high-resistance line is used to form a coil that is evenly distributed over the full length of the toroid. The transfer impedance of these current probes (ratio of output voltage to measured current) is typically about 6 ohms at 1 MHz, and increases by 20 dB per decade of frequency. In each of these probes the signal is rectified by a diode located at the terminals of the winding, and resistive line is used to connect the direct current (DC) output of the probe to (high-impedance) readout electronics.

High-permeability cores are not used in our current probes since we have shown analytically (See Section 7), as well as by experiment, that a probe can function properly (output proportional to the total current passing through the aperture and independent of the spatial distribution of the current) without them. We have shown that when a ferromagnetic core is not used, it is necessary to have the coil winding distributed over the full length of a toroidal core. The product of the number of turns per unit length of the winding and the cross-sectional area of the toroid must be kept constant over the full length of the coil. Use of a low-permeability core has the disadvantage that it reduces the transfer impedance (sensitivity), but it reduces field perturbations, permits greater bandwidth, and avoids errors due to nonlinearity and possible saturation of the core since the permeability is an exact constant.

Open field tests were made previously, in which our current probes were used for fixed-frequency measurements with a man-sized phantom at the Naval Aerospace Medical Laboratory (NAMRL) in Pensacola, Florida [1],[4]. The phantom was positioned so it was standing on a metal ground plane 1 m from a 10-m vertical monopole antenna, and a power of 1 kW at 29.9 MHz was fed to the antenna. A Bowman temperature probe was used to determine the local specific absorption rate (SAR, the rate of energy deposi-

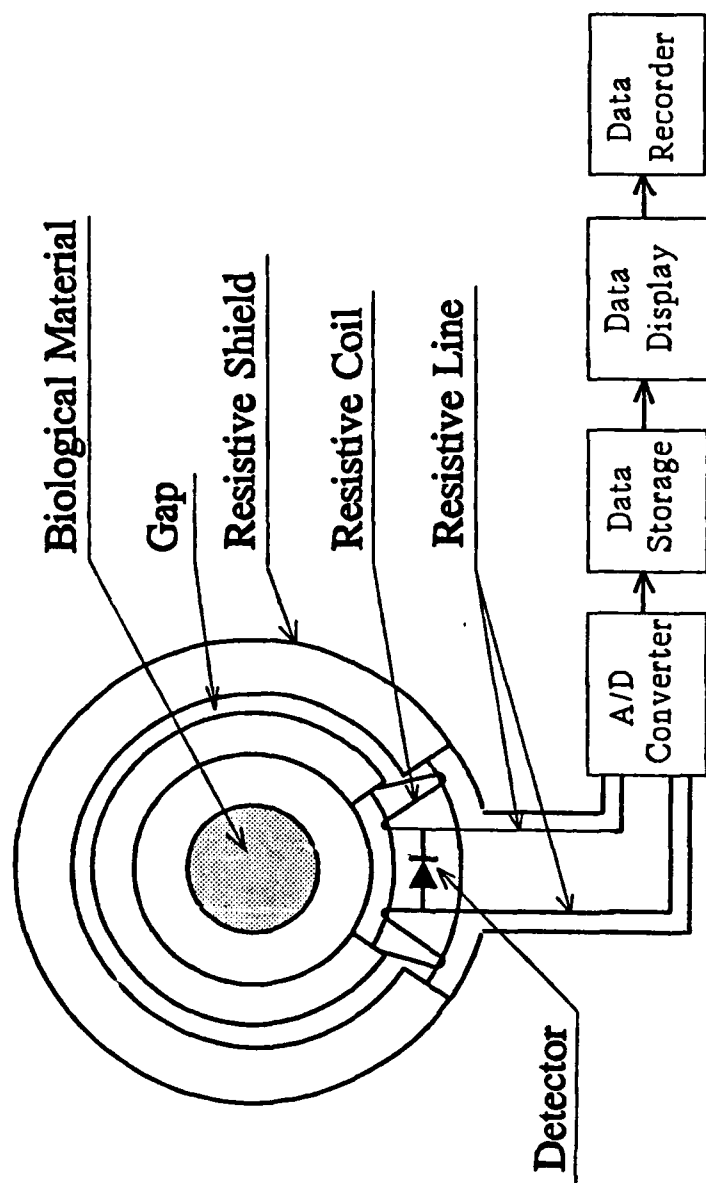


Figure 1. Block diagram of new current probe.



tion per unit mass) at a point 27 cm above the ground plane on the axis of one leg of the phantom. One of our current probes was used to simultaneously measure the current in the leg. This experiment was made for both the arms raised (SAR = 4.4 W/kg, current = 517 mA) and the arms lowered (SAR = 2.8 W/kg, current = 448 mA). Using published values for the dielectric properties of the phantom, the SAR calculated from the measured currents differs from the value determined with the Bowman probe by -9.1 % for the arms raised and +7.1 % for the arms lowered.

The current probes used in the fixed-frequency measurements at NAMRL are toroidal in shape, with an aperture radius of 9 cm and an outer radius of 11 cm (tube radius of 1 cm). The winding of 150 turns of high-resistance line is evenly distributed over the full length of the toroid, the total resistance being 500 kohms. At frequencies below the coil resonance (100 MHz), the output of these probes (V) is related to the time derivative of the measured current (A/ns) by  $V = 94.2 \text{ dI/dt}$ .

The minimally perturbing current probes for fixed-frequency measurements, which we developed previously, are not suitable for time-domain measurements in EMP simulations. Major design changes were required to produce the following five changes in operating characteristics:

(1) Increased Bandwidth; Greater bandwidth is required so that the time-dependent (unrectified) output can be used to determine the instantaneous value of current. Numerical simulations of human exposure to VPD by Guy [11] suggest that the 3 dB points for current occur at 0.7 and 40 MHz.

(2) Increased Ruggedness; Greater electronic ruggedness is required because of the high intensity of EMP fields.

(3) Decreased Output Impedance; The time-dependent (unrectified) output of the probe should be compatible with a low-impedance (50 ohms) fiber-optics transducer for data acquisition, rather than high-impedance readout electronics.

(4) Decreased RFI Susceptibility; Improved shielding is required because of the high intensity of EMP fields.

(5) Decreased Sensitivity; Calculations suggest that the peak current induced in man due to exposure to 100 kV/m EMP with a VPD may be as large as 500 A [11]. The peak value of the rate of change of current in the human leg was reported as 2.1 A/ns for VPD exposure [9]. The current probes we used at NAMRL have a sensitivity of 94.2 V per A/ns, so the unrectified output of a probe would be approximately 200 V which would overload the fiber-optics transducer.

### 3. CALIBRATION PROCEDURES

Early in this project we recognized that carefully defined calibration procedures are essential for characterizing a particular current probe, as well as determining the effects of various design parameters for probe optimization. We had several phone conversations with engineers at the Eaton Corporation to determine the methods used to calibrate commercial current probes, and have used these procedures with each of the new probes. We have also developed new shielded test fixtures which we consider to be more practical and give higher accuracy than those used previously by others. We have also used loop test fixtures and have found they can detect anomalous probe responses which are missed using the standard shielded test fixtures.

#### Standard Shielded Test Fixtures

We have followed the procedures used to calibrate commercial current probes at the Eaton Corporation in characterizing each of the new current probes. We fabricated shielded test fixtures to those at Eaton and verified that our calibrations of 3 commercial current probes agree with measurements made by the manufacturer.

These shielded test fixtures are rectangular metal boxes with coaxial connectors at the centers of the tops and bases, and metal cylinders join the center pins of the 2 connectors. The box and center conductor form a coaxial transmission line, and a current probe is placed in the box with the center conductor passing through the probe window. Engineers at Eaton recommend that the voltage standing-wave ratio (VSWR) of a loaded test jig be less than 2.0.

A current probe is placed in the test fixture, and 50 ohm coaxial cable is used to connect one terminal to a signal generator and the other to a detector such as an oscilloscope. It is necessary to match the detector to the fixture, so if an oscilloscope is used, it is necessary to have a T with a 50 ohm shunt at the scope. The voltage across the load is measured to determine the current through the probe aperture. At a fixed frequency, the transfer impedance of the probe is calculated by dividing the total voltage output of the probe by the current. A two-port network analyzer, measuring input current and output voltage simultaneously, is the preferred way of making the measurement.

#### New Shielded Test Fixtures

We have developed new shielded test fixtures that are more practical to use with our current probes than the standard shielded test fixtures described in the previous section of this report. The new test fixtures consist of 2 flat metal sheets, each with a coaxial connector at the center, and a metal cylinder

joining the center pins of the 2 connectors. The 2 metal sheets are placed across the top and base of the aluminum shield of a current probe, and the metal cylinder and the inner surface of the shield form a coaxial transmission line. The diameter of the metal cylinder is chosen so that the characteristic impedance is about 50 ohms. One Model 10 test fixture has been supplied as a part of this project.

The characteristic impedance of the shielded test fixtures is determined by the ratio of the diameter of the center conductor to (1) the diameter of the aperture of the current probe in the new fixtures, and (2) the size of the metal box in the standard fixtures. Objects placed in a Crawford cell should be smaller than one-third the cross-section of the cell to limit perturbations of the field distribution and an unacceptable increase in the VSWR. We believe that a similar specification should be followed with shielded test fixtures because they are transverse electromagnetic (TEM) devices closely related to the Crawford cell. If the box in a standard test fixture is large enough to meet this specification for a current probe, then, in general, a center conductor which will fit through the window of the probe is too small for a characteristic impedance of 50 ohms. Thus, we find that a VSWR of less than 1.1 (0.4 to 110 MHz) may be obtained with the new shielded test fixtures, as compared to a value of 2.0 for the standard shielded test fixtures.

#### Loop Test Fixtures

Two types of loops have also been used as test fixtures with the new current probes. One is a simple loop in which the center conductor of a section of 50 ohm coaxial cable is bent so that it returns to make electrical contact with the outer conductor through a 50 ohm resistor. The second is a shielded loop in which the entire coaxial cable is bent so that it returns on itself, and both the center and outer conductor at the end of the cable are soldered to the outer conductor. A gap is made in the outer conductor at the center of the circular loop. Both types of loops are made as small as possible, while interlacing through the aperture (window) of the current probe, to increase the upper usable frequency for the system to about 100 MHz.

We use the 2 types of loops to detect possible changes in the sensitivity of a current probe when the source current is at different locations in the probe window. The 2 types of shielded test fixtures described in the previous sections give an integrated measurement of the sensitivity.

We believe that calibrations with shielded test fixtures may not properly represent the conditions under which current probes are used and recommend that the loops or other unshielded test fixtures be used to supplement the calibration data. We have found anomalous responses in several commercial current probes

when they are tested with the loops, even though we were able to duplicate the calibration curves from the manufacturer by using our shielded test fixtures. The magnetic field in a shielded test fixture is primarily due to the current in the conductor passing through the probe window. The electrostatic shield of a current probe limits the sensitivity to electric fields. Thus, a current probe in a shielded test fixture responds primarily to the magnetic field produced by the current passing through the probe window. A more complex field pattern, more closely related to common usage of the probes, is presented by the loop test fixtures.

#### 4. RFI SUSCEPTIBILITY

Early in this project it was recognized that methods for determining RFI susceptibility must be carefully defined before characterizing a particular current probe or determining the effects of various design parameters for probe optimization. We have developed our own methods for determining RFI susceptibility of current probes because our test results suggest that the procedures used to test commercial current probes are often inadequate.

We have evaluated the RFI susceptibility of the new current probes as well as several commercial current probes using (1) loop test fixtures that do not interlace the probes, (2) a Crawford cell, and (3) a simple parallel plate fixture.

##### Decreasing RFI Susceptibility of the New Probes

Pickup through the electrostatic shield may be eliminated by using care in the fabrication of the shield. It is necessary to inspect for flaws in the shield and to use care in designing the circumferential gap.

The RFI susceptibility of our new current probes is mostly due to cable pickup. As with commercial probes, this problem may be minimized by using (1) short cables, (2) ferrite beads to load the cable shield, (3) double-shielded cable, and (4) other standard procedures.

The toroidal winding in each of the new current probes is a symmetrical device, so balanced loading is required to minimize RFI and other extraneous responses of the probe. When using a probe with a detector having an unbalanced input, such as a fiber-optic transducer in field tests or an oscilloscope in bench top testing, each terminal of the winding must be connected to a separate channel of the detector. The electrostatic shield of the current probe is connected to the cable shields, and hence to the ground of the detector. In some models of the new current probes, we have used Twinax cable, in place of two separate

cables, and have found that this reduces the effects of cable pickup.

Each of our Model 12 current probes, supplied as a part of this project, has two type N connectors, one for each end of the internal coil. Both of these outputs should be matched by 50 ohm loads. The probes are designed to be compatible with low-impedance (50 ohms) fiber-optic transducers typically used for data acquisition in EMP simulations. When a probe is used with an oscilloscope, it is necessary to have a T with a 50 ohm shunt at both inputs of the oscilloscope for proper matching to the probe. When a single channel detector must be used, then a 50 ohm load should be connected to the unused output of the probe. If a current probe is not properly loaded, mismatch causes a change in both the frequency response and the sensitivity.

#### RFI Susceptibility of Commercial Current Probes

We tested an Eaton Model 93686-4 current probe and found it to be highly susceptible to RFI. When this probe was placed in a Crawford cell, and exposed to approximate TEM fields but no current, the ratio of probe output to the current input to the cell exceeded the specified transfer impedance at frequencies greater than 30 MHz. This anomalous response of the probe was not apparent in calibration using a shielded test fixture. We found an apparent design error in the current probe. The paint on the electrostatic shield was not removed beneath the type N connector, and there is a gap between the connector and the shield. The RFI susceptibility of the probe was decreased by about two orders of magnitude by closing this gap with pressure-sensitive copper tape.

### 5. MODIFICATIONS OF THE CURRENT PROBES

#### Electrostatic Shield

An electrostatic shield is essential to limit capacitive coupling so that the current probes operate properly. When one of the current probes is tested without an electrostatic shield, the probe has an output due to the TEM fields of a Crawford cell, even though no current passes through the probe window. An unshielded probe also responds to a loop test fixture, even when the loop does not interlace the probe. Also the output from the probe is changed by bringing the hand near the probe during measurements. These extraneous responses are eliminated by using the electrostatic shield.

It would be ideal to use a resistive shield to minimize the field perturbations caused by a current probe. We tested probes using several materials including Teledeltos paper and carbon loaded plastic for resistive shields, but found that these mate-

rials have specific resistivities that are too high to provide adequate RFI susceptibility for use in EMP simulations, so we have chosen to use metal shields instead.

The electrostatic shield, which is the outer aluminum container of the current probe, must be carefully sealed to limit capacitive coupling and RFI. Copper or aluminum pressure-sensitive tape is used to seal all gaps in the shield, except for the circumferential gap on the inner surface of the probe which must be kept open at all times to permit coupling to the magnetic field produced by the source current.

### Coil Resistance

We have used distributed resistive loading to decrease the quality factor of the coil in each current probe to obtain greater bandwidth. A number of probes were constructed with different values of coil resistance, and we determined the effects of coil resistance on some of the characteristics of the probes. The final probes have a coil resistance of 30 to 40 kohms, which is a compromise providing (1) adequate bandwidth, and (2) low enough attenuation that the output of the probe is not sensitive to the position of the current within the probe aperture.

Since the coil is resistively loaded, there is some attenuation in propagation on this coil, so the output of a probe is greatest if the current is near the end of the probe where the connectors are located. The dependence of probe output on location of the current is only pronounced when the current is close to the metal shield, so this undesirable effect may be minimized by using a spacer of Styrofoam or other low-density low-loss dielectric to keep the leg, or other current-carrying part, at least 1 to 2 cm from the inner surface of the shield. We have evaluated the dependence of probe output on location of the current by using the loop test fixtures described in section 3 of this report.

We have formed the resistive winding for each probe by using a large number of carbon resistors connected in series, so that there is about one per turn. The Model 12 series probes use 150 ohm 1/8 Watt, carbon film resistors (probe with serial number 1 has 200 turns and total resistance of 33.2 kohms; Probe with serial number 2 has 225 turns and total resistance of 36.6 kohms). We have used resistance wire and carbon-loaded plastics in some coils, but find that they are not practical for the value of ohms per unit length that is optimum for the probes (e.g., too small a diameter of wire and too large a diameter of carbon-loaded plastic).

If a conductive coil were used in place of a resistively loaded coil, the field perturbation would not be measurably increased because the coil is contained in a metal electrostatic

shield. The coil and shield act as a coaxial transmission line so in principle, broad bandwidth could be obtained with a conductive coil if this line was matched by loads at both ends of the coil. We have made several tests which suggest that it may be possible to obtain adequate bandwidth without resistive loading.

The output impedance of the probe was specified to be 50 ohms to match the input of the fiber-optic systems used for data acquisition in EMP measurements. We have found it is possible to decrease the characteristic impedance of the coil/shield transmission line (See Section 7) to about 50 ohms by using a metal tape helical toroid winding with a closely spaced shield. The VSWR for the modified probe, loaded by 50 ohms, is less than 1.2 from 0.4 to 110 MHz. This design offers a number of advantages over the probes we have used so far, but it is still in a developmental stage so probes with resistive windings were furnished by us on the present contract.

#### Increasing Bandwidth

We have chosen to use no active elements (amplifiers, active filters, etc.) to decrease the possibility of burnout in the intense fields of an EMP simulator. From Faraday's law of induction, we see that at frequencies below coil resonance (100 MHz) the output of a current probe is proportional to frequency. The effects of coil resonance have been damped by resistive loading, and the flatness of response has been improved by adding a low-pass filter.

The low-pass filter used with the current probes consists of a shunt capacitor, in combination with the series resistance of the coil. This filter causes the response to be relatively flat from the cutoff frequency of the filter,  $f_c$ , to about 100 MHz, by decreasing the sensitivity at higher frequencies to that at  $f_c$ . We have chosen to use a shunt capacitor of 220 pF, which is a compromise between bandwidth and sensitivity. The manual supplied with each probe has tables and figures giving the transfer impedance as a function of frequency both with and without the shunt capacitor. The shunted probes have decreased sensitivity, but are considered adequate for use in EMP simulations, because the peak current induced in man due to exposure to 100 kV/m is about 500 A [11].

#### Description of the Completed Probes

The new current probes are designed for noninvasive measurement of current in personnel exposed to EMFs, with particular emphasis on the pulsed fields in EMP simulations. The Model 12 series probes are toroidal in shape, with an inner radius of 10.8 cm, outer radius of 15.2 cm, and a height of 4.8 cm. This size is suitable for placement on the human thigh, even with most endomorphic or mesomorphic people. The transfer impedance is

typically 1.90 mohm/MHz +/- 12 percent in the frequency range of 1 to 200 MHz. Full descriptions of the probes and instructions for their use are contained in the manuals supplied with the probes.

## 6. INSERTION IMPEDANCE OF CURRENT PROBES

We have shown by analysis and experiments that both the ferromagnetic core and the grounded metal shield of a current probe modify the circuit in which the probe is used by introducing an insertion impedance, thus changing the current being measured. The ferromagnetic core introduces a series inductance into the circuit, and the grounded metal shield introduces a capacitive shunt to ground.

Antenna theory has been used previously to determine the SAR for models of man in free-space as well as with ground and reflector effects [12]. We model the human body with a vertical cylindrical monopole antenna above ground. The cylinder has a length of 175 cm, the height of the standard man, and a radius of 11.3 cm, for a volume corresponding to 70 kg of tissue. The current probe is modeled by adding a series inductance and a capacitive shunt to ground.

We have determined the value of the series inductance added by the ferromagnetic core of the current probe by (1) using the total current, conduction plus displacement, with Ampere's Law to calculate the magnetic field intensity, (2) integrating to find the total magnetic energy, and (3) relating the total magnetic energy to inductance and current. Our calculations have shown that in biological applications this inductance may be as much as 1 mH since a large fraction of the aperture is filled, but the effect is often negligible with a wire conductor (for which the probes were intended).

The grounded metal shield introduces a capacitive shunt to ground. This capacitance was determined with the expression for a coaxial transmission line, which neglects fringing which occurs if the gap between the probe and the antenna is not much smaller than the length of the probe. Our calculations have shown that in biological applications the value may be as much as 100 pF when the shield is close to the body, but the effect is often negligible with a wire conductor (for which the probes were intended).

The reactance of the antenna model was determined using the approximation of open-ended, tapered, two-wire transmission line, and changes in reactance due to the current probe were calculated. Resonances without the probe were at 43 and 86 MHz. Our calculations suggest that when a probe having inner radius of 12.3 cm, outer radius of 14.3 cm, length of 2.0 cm, and relative



permeability of 4000 is added at a height of 24 cm above ground, the resonances are shifted to 16, 40, 54 and 86 MHz.

We have also determined the insertion impedance of several commercial current probes by measuring the impedance of a test fixture consisting of an aluminum cylinder 3.1 cm in diameter and 28 cm long, which was connected to a Hewlett Packard 4193A Vector Impedance Meter with two-wire transmission line. The impedance of this circuit, both with and without current probes, was measured from 0.5 to 110 MHz. The data in Table I show that significant changes in impedance occur when either of two commercial current probes is placed on the cylinder. The aperture diameter is 3.5 cm for the Eaton Model 91550-1 probe, and 6.5 cm for the Eaton model 93686-4 probe. The Eaton model 93686-4 probe has a larger diameter, so less of the aperture is filled by the cylinder, but this probe is more massive than the 91550-1; hence, the two probes have similar effects on the circuit. At frequencies near resonance, the impedance (and, hence, the current) in this circuit is typically changed by approximately one order of magnitude when either current probe is placed on the cylinder. We observed that the effects of two probes are not additive, which may be explained by capacitive shunting of the probe nearer ground.

Table I. Measurements of Impedance

	No Probe	Eaton 91550-1	Eaton 93686-4
First Resonance	51.53 MHz 5.3 kohm	49.76 MHz 3.7 kohm	50.42 MHz 3.7 kohm
Second Resonance	77.03 MHz 34 ohm	74.24 MHz 28 ohm	73.38 MHz 26 ohm
Third Resonance	92.49 MHz 1.7 kohm	92.70 MHz 2.0 kohm	92.31 MHz 2.1 kohm

Our experiments have also shown that the ferromagnetic core of a current probe increases the circuit resistance, and that the insertion impedance is primarily resistive at frequencies below 100 MHz. Apparently the depth of current flow in a conductor is reduced by the presence of the ferromagnetic core, thus causing the circuit to have increased resistance. Our new current probes, not having ferromagnetic cores, cause significantly less insertion impedance than the commercial current probes which we have tested.

## 7. ANALYSIS OF CURRENT PROBES

### Commercial Current Probes

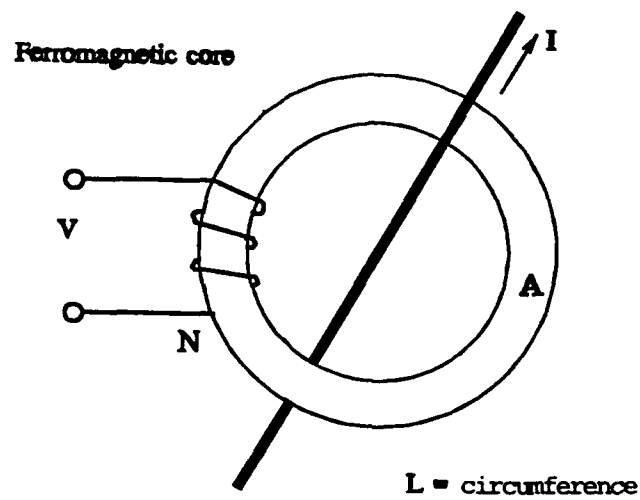
Commercial current probes use a ferromagnetic core to couple the magnetic flux produced by the current to a coil, and the voltage induced in this coil is measured to evaluate the current. A derivation showing how these probes function is given in Fig. 2. This derivation may be summarized as follows:

The ferromagnetic core has a permeability much greater than that of the surrounding medium, so the boundary relations for magnetic fields require that the magnetic flux within the core is independent of azimuthal location. The permeability and cross-sectional area  $A$  of the core are constant, so the magnetic field intensity  $H$  has a constant magnitude within the core and is oriented azimuthally. Thus, Ampere's Law requires that this value of  $H$  is equal to the total current passing through the aperture of the core, divided by the circumference of the core. Therefore, the magnetic flux and, hence, the voltage output of the probe is independent of the distribution of current within the aperture. Note that the coil may be located anywhere on the core because the flux is independent of azimuthal location. Furthermore it is not necessary that the axis of the core be circular in shape. Inspection of the equations shows that neither the cross-sectional area nor the permeability need be constant, but their product must be constant over the length of the core.

### Non-Ferromagnetic Probe with Axial Current

High-permeability cores are not used in our current probes. The derivation in Fig. 3 shows that a uniformly wound toroidal coil has a voltage output proportional to the current, if the current is on the axis of the coil. This derivation may be summarized as follows:

Since a ferromagnetic core is not used, it is no longer possible to use boundary relations, as in the previous derivation, to show that the magnetic flux within the core is independent of azimuthal location. However, if the current is on the axis of the toroid, Ampere's Law requires that the magnitude of  $H$  is constant (the current divided by the circumference of the core) within the coil. If the coil winding is distributed over the full length of a toroidal core, and the number of turns per unit length and the cross-sectional area  $A$  are constant, then the potentials from each increment in length of the coil may be summed to give an equation relating voltage output to current that is the same as in the previous derivation for a ferromagnetic core. Inspection of the equations shows that neither the number of turns per unit length nor the cross-sectional area need be constant, but their product must be constant over the length of the coil.



Ampere's law

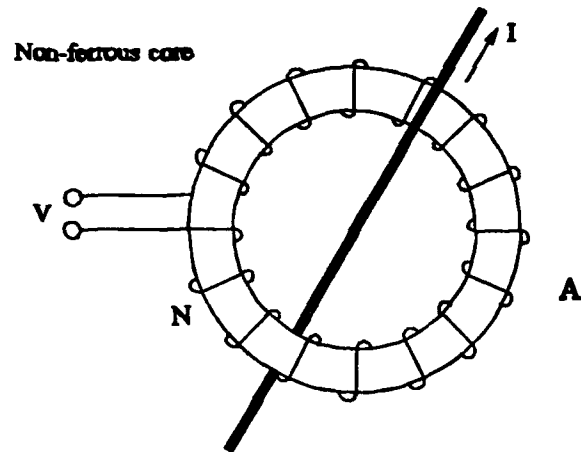
$$\oint \vec{H} \cdot d\vec{l} = I$$

$$\phi = \frac{\mu AI}{L}$$

$$V = - \frac{j\omega \mu N A I}{L}$$

Coil may be anywhere on the core

**Figure 2. Derivation for ferromagnetic current probe.**



At any azimuthal location on the coil

$$\phi = \mu A \vec{H} \cdot \hat{I}$$

$$dv = -j\omega\phi \left( \frac{N}{L} dl \right) = -\frac{j\omega\mu NA}{L} \vec{H} \cdot d\vec{l}$$

$$v = -\frac{j\omega\mu NA}{L} \oint \vec{H} \cdot d\vec{l}$$

Using Ampere's law

$$v = -\frac{j\omega\mu NA I}{L}$$

Turns per unit length  $\times$  area = Constant

**Figure 3. Derivation for non-ferrous current probe.**

### Non-Ferromagnetic Probe with Off-Axis Current

It is possible to show that the relationship of the voltage output to the input current is unchanged if a current filament has an arbitrary location within the aperture of the toroid, and that the output is zero if the current filament is outside of this aperture. This derivation is more complicated than that in Fig. 2 because a ferromagnetic core is not used, so the magnetic flux is not constant from point to point within the coil. Furthermore, since the current filament is not on the axis of the toroid (as it is in Fig. 3), the magnetic field intensity does not have constant magnitude within the toroid and is not oriented orthogonal to the plane of each turn of the toroid. In the following derivation, we refer to the parameters defined in Fig. 4.

In the triangle in Fig. 4, the following trigonometric relations may be used:

$$s^2 = r^2 + d^2 - 2rd \cos \theta \quad (1)$$

$$\frac{s}{\sin \theta} = \frac{d}{\sin \alpha} \quad (2)$$

From (1) and (2) we obtain

$$\cos \alpha = \sqrt{1 - \frac{d^2}{s^2} \sin^2 \theta} \quad (3)$$

From (3) we obtain

$$s \cos \alpha = \sqrt{r^2 + d^2 - 2rd \cos \theta - d^2 \sin^2 \theta} \quad (4)$$

which simplifies to

$$s \cos \alpha = r - d \cos \theta \quad (5)$$

From (1) and (5) we obtain

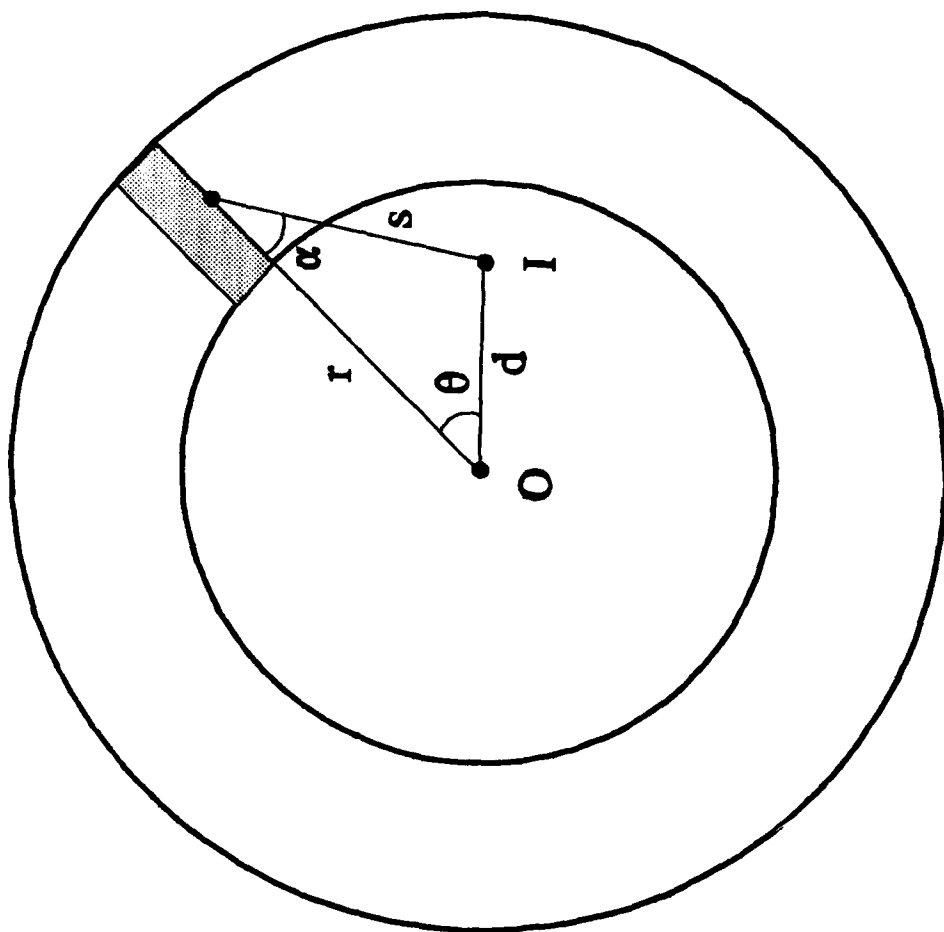


Figure 4. Non-ferromagnetic core with an off-axis current filament.

$$\frac{\cos \alpha}{s} = \frac{r - d \cos \theta}{r^2 - 2rd \cos \theta + d^2} \quad (6)$$

The magnitude of the magnetic field intensity at the center of the shaded increment of winding is given by

$$H = \frac{I}{2\pi s} \quad (7)$$

Thus, the value of the magnetic field intensity perpendicular to the increment of winding is given by

$$H_p = \frac{I \cos \alpha}{2\pi s} \quad (8)$$

From (6) and (8) we obtain

$$H_p = \frac{I}{2\pi} \left( \frac{r - d \cos \theta}{r^2 - 2rd \cos \theta + d^2} \right) \quad (9)$$

The number of turns on the increment of winding is given by

$$dn = \frac{n d\theta}{2\pi} \quad (10)$$

Using Gauss's Law with (9) and (10), the voltage on the increment of winding is given by

$$dv = \frac{\mu_0}{2\pi} \left( \frac{r - d \cos \theta}{r^2 - 2rd \cos \theta + d^2} \right) \left( \frac{dI}{dt} \right) A dn \quad (11)$$

Thus integrating over the length of the coil, the total voltage is given by

$$V = \frac{\mu_0 n A}{(2\pi)^2} \left( \frac{dI}{dt} \right) \int_0^{2\pi} \left( \frac{r - d \cos \theta}{r^2 - 2rd \cos \theta + d^2} \right) d\theta \quad (12)$$

We normalize the integrand in (12) to obtain

$$V = \frac{\mu_0 n A}{L} \left( \frac{dI}{dt} \right) \int_0^{2\pi} \left( \frac{1 - \frac{d}{r} \cos \theta}{1 - \frac{2d}{r} \cos \theta + \frac{d^2}{r^2}} \right) \left( \frac{d\theta}{2\pi} \right) \quad (13)$$

This integral has the following values:

$$\begin{aligned} -1 & \text{ for } \frac{d}{r} > 1 \\ \frac{1}{2} & \text{ for } \frac{d}{r} = 1 \\ 0 & \text{ for } \frac{d}{r} < 1 \end{aligned} \quad (14)$$

Thus, there is no output if the current filament is outside of the aperture of the toroid, and for an arbitrary location within the aperture the voltage is given by

$$V = \frac{\mu_0 n A}{L} \frac{dI}{dt} \quad (15)$$

Inspection of the above derivation shows that neither the number of turns per unit length nor the cross-sectional area need be constant, but their product must be constant over the length of the coil. Furthermore, it is possible to extend the derivation to show that the axis of the coil need not be circular in shape.



The derivations presented thus far in this section are only valid at low frequencies. Furthermore, they are for current filaments rather than currents in lossy biological tissues. In general, it is necessary to allow for retarded times and attenuation during propagation from the source current to the coil and for delays and attenuation during propagation on the coil. Some of the effects due to propagation on the coil will be treated in the following part of this section.

### Probe Coil/Shield as a Transmission Line

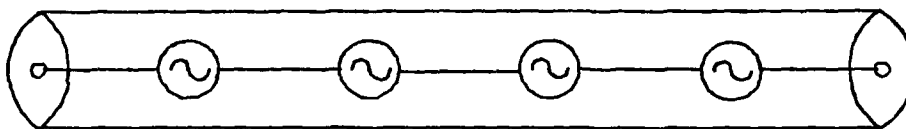
Since the new current probes do not have ferromagnetic cores, the coil winding must be distributed over the full length of a toroid, instead of using a short coil such as in the commercial probes. Thus, the induced voltage is distributed over the full length of the coil, rather than being a localized source. It was necessary to use a distributed voltage source in the derivations for Figs. 3 and 4 referred to in the previous parts of this section. The continuous distribution of induced voltage over the length of the coil may be approximated by a finite number of discrete sources as shown in Fig. 5A. The coil and shield form a coaxial transmission line, and the voltage is induced in the coil which is the inner conductor of this line.

The response of the new current probes may be evaluated by determining how the distributed voltage source is combined to yield the output of the probe. The derivations in Figs. 3 and 4 assumed that the output is a simple summation of increments of the distributed voltage source, but this approximation is only valid at low frequencies. At high frequencies it is necessary to allow for the effects of the coil/shield transmission line on this summation.

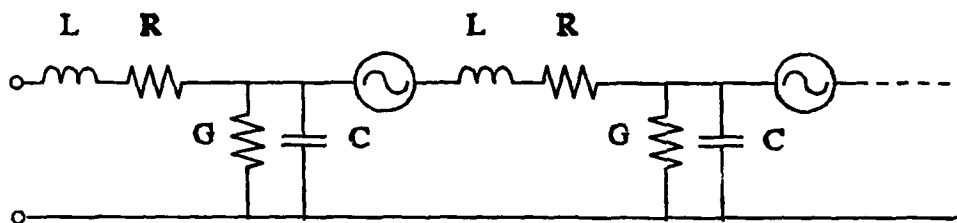
The characteristics of a uniform transmission line may be determined using an equivalent circuit [13] consisting of 4 distributed quantities: (1) the series resistance  $R$  ohm/m, (2) the series inductance  $L$  Henrys/m, (3) the shunt capacitance  $C$  Farads/m, and (4) the shunt conductance  $G$  Siemens/m. It is possible to determine how the distributed voltage source yields the output of a current probe by adding the RLCG models to Fig. 5A, to represent sections of the coil/shield transmission line coupling the discrete voltage sources, thus forming Fig. 5B.

Figure 5C is the final model which we have used to analyze the new current probes. This model differs from Fig. 5B showing that: (1)  $R$  and  $L$  are due to the resistively loaded coil, (2)  $C$  is due to the capacitance between the coil and the shield, (3)  $G$  may be neglected because low-loss dielectrics are used, and (4) the discrete voltage sources are located in the coil. Values of the distributed quantities  $R$ ,  $L$ , and  $C$  may be measured for a current probe, and used to evaluate the (complex) characteristic

A.)



B.)



C.)

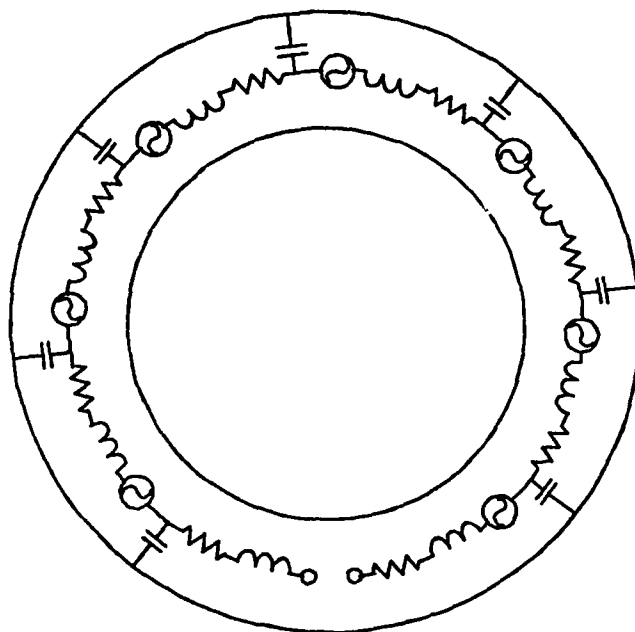


Figure 5. Transmission line model of the probe coil shield.

impedance, phase velocity and attenuation [13]. We have found this procedure to be useful in explaining the frequency response of the new current probes and in the optimization of these probes. In commercial current probes the shield is only needed to limit capacitive coupling, but in the new probes the shield is a part of a coaxial transmission line and is essential to the operation of the devices at high frequencies.

## 8. FIELD TESTING AT THE ALECS FACILITY

Our new non-ferrous current probes were tested at the Air Force Los Alamos Laboratory Electromagnetic Pulse Calibration and Simulation (ALECS) facility, at Kirtland AFB, on April 29 to May 2, 1991, as a part of this project. This is a VPD system.

First, our non-ferrous current probes and an Eaton Model 94456-2 ferrous current probe were successfully interfaced with the ALECS measurements system. The non-ferrous probes have a balanced 50-ohm output, which is compatible with the fiber optic link used at ALECS. Each of the two connectors on our probes was connected to the fiber-optic link using differential mode. In order to have data manipulation consistent with the ALECS system it was necessary to sweep each probe to determine the transfer impedance as a function of frequency and then use this transfer function to correct for frequency dependence. For each test, it was necessary to (1) record the digitized output of the probe in the time domain, (2) take a Fourier transform of this record, (3) multiply the (frequency domain) transform by the transfer function for the system (including cables, etc., as well as the probe), and (4) take an inverse Fourier transform to obtain the corrected waveform for current in the time domain.

Table II gives the values of currents measured with our non-ferrous probe (NF) and the Eaton probe. We report values of the extreme peak-to-peak currents found in the reduced time-domain data in order to have a single number representing the current in each test. Values of the extreme positive and extreme negative current were less reproducible than the peak-to-peak measurement. The shot numbers are tabulated to permit referencing the stored data at the ALECS facility. Tabulated electric field values were measured near the subjects.

In order to limit the use of human volunteers, preliminary testing was made using a 3 m vertical grounded cable as the subject. A non-ferrous current probe and the Eaton probe were both near the ground end of the cable. Current values for the first three shots reported in Table II show that when the cable is used, the two probes give similar results. A human volunteer was used in each of the 17 remaining tests in Table II.

A human volunteer, standing with arms at the sides, was used in tests 4732-4737 of Table II. For each of these tests, the two current probes were on the right ankle of the subject. The mean field strength for these 6 tests is 48.6 kV/m, and the mean values of peak-to-peak current are 136 A with the non-ferrous probe and 122 A with the Eaton probe.

Table II. Summary of Measurements at the ALECS Facility

Shot	Field kV/m	Peak-to-Peak Current, A		Conditions of Test
		NF Probe	Eaton Probe	
4725	14.5	98.	99.	10 m vertical cable
4729	45.7	310.	315.	10 m vertical cable
4730	46.8	300.	340.	10 m vertical cable
4732	49.7	130.	130.	Both probes on rt. ankle
4733	48.8	122.	103.	Both probes on rt. ankle
4734	48.2	148.	135.	Both probes on rt. ankle
4735	49.6	138.	155.	Both probes on rt. ankle
4736	47.3	146.	100.	Both probes on rt. ankle
4737	47.7	130.	108.	Both probes on rt. ankle
4738	48.5	228.	194.	NF on thigh, Eaton ankle
4739	48.6	223.	204.	NF on thigh, Eaton ankle
4740	49.4	234.	164.	NF on thigh, Eaton ankle
4741	47.9	92.	132.	Both probes on rt. ankle
4742	47.3	101.	110.	Both probes on rt. ankle
4743	47.9	107.	113.	Both probes on rt. ankle
4744	47.1	103.	...	NF on right ankle
4745	47.2	106.	...	NF on right ankle
4746	46.0	124.	108.	Both probes on rt. ankle
4747	47.5	57.	21.	NF on shoulder, Eaton on arm
4748	48.2	52.	26.	NF on shoulder, Eaton on arm

The human volunteer had his left leg raised, and both arms vertical above the head, for tests 4738-4740. The non-ferrous current probe was on the right thigh, and the Eaton probe on the right ankle. Raising the arms increased the current, as would be predicted from antenna theory [12]. Raising the left leg forced the total current to pass to ground through the right leg, where current was measured. Thus, this posture for the subject is regarded as a "worst case," maximizing the measured currents. The mean field strength for these 3 tests is 48.8 kV/m, and the mean values of peak-to-peak current are 228 A at the thigh, and 187 A at the ankle. The current is significantly greater at the thigh than at the ankle, and this variation would be missed in a measurement involving only foot current.

The human volunteer was again standing with arms at the sides (as in tests 4732-4737) for tests 4741-4746 of Table II. Both current probes were on the right ankle in tests 4741-4743 and 4746, and the ferrous current probe was removed in tests 4744-4745. The objective of this series of 6 tests was to determine if the ferrous current probe changes the current in the human subject. We conclude that there was no significant change in the reading of our non-ferrous probe due to the ferrous probe in these data, but a definitive answer cannot be given due to the variability from shot to shot, which is attributed to variations in the pulse.

The human volunteer again stood with arms at the sides for the last two tests (4747-4748). The non-ferrous current probe was on the left shoulder of the subject, and the Eaton probe was on the right upper arm. The data show that the current is much lower in the shoulders and arms than in the legs for VPD.

## 9. FIELD TESTING AT THE EMPRESS I FACILITY

Our new non-ferrous current probes were tested at the Electromagnetic Pulse Radio Environment Simulator for Ships (EMPRESS) I facility, in Solmons, Maryland, on October 21-24, 1991, as a part of this project. This is a VPD system.

First our non-ferrous current probes, and an Eaton Model 94456-2 ferrous current probe, were successfully interfaced with the EMPRESS I measurement system. At this facility, unlike ALECS, it was not possible to use the fiber-optic link in a differential mode, so it was necessary to use an EG&G DMB-1A BALUN to transform the balanced output of our non-ferrous probes to the unbalanced input of the link. Also, it was not practical to use the data reduction procedures used at ALECS, since there was no provision for taking Fourier transforms to the site. Thus it was necessary to use an EG&G ODT-6E fiberoptic transmitter that has a built-in integrator. Our non-ferrous probes have a transfer impedance proportional to frequency, as required by Faraday's Law of induction, so the integrated output is nearly flat from 1 to 200 MHz.

Table III gives the values of currents measured with our non-ferrous probe (NF) and the Eaton probe. We report only the peak current in each case. The shot numbers are tabulated to permit referencing the stored data at the EMPRESS I facility. Tabulated electric field values were measured near the subjects with a D-dot probe used at the facility.

In order to limit the use of human volunteers, preliminary testing was made using a 3 m vertical grounded copper pipe as the subject. A non-ferrous current probe and the Eaton probe were both on the pipe at a distance of 1 m above the ground. For the first three shots reported in Table III, the mean values of the peak current are 80.4 A with the non-ferrous probe and 77.2 A with the Eaton probe. While there is considerable scatter, these mean values do not suggest that there is a significant difference between the two probes.

A human volunteer, standing with arms at the sides, was used in tests 24-28 of Table III. The subject was 32 m from the center of the simulator, and faced this center. For each of these tests, the two current probes were on the right ankle of the subject. The mean field strength for these 5 tests is 28.1 kV/m, and the mean values of peak current are 26.4 A with the non-ferrous probe and 37.7 A with the Eaton probe.

Table III. Summary of Measurements at the EMPRESS I Facility

Shot	Field kV/m	Peak Current, A		Conditions of Test
		NF Probe	Eaton Probe	
17	29.1	75.1	82.8	10 m vertical pipe
21	28.0	81.9	72.5	10 m vertical pipe
22	28.3	84.3	76.4	10 m vertical pipe
24	28.9	26.1	38.2	Both probes on rt. ankle
25	27.7	27.1	36.7	Both probes on rt. ankle
26	27.7	27.1	36.3	Both probes on rt. ankle
27	27.7	25.0	39.1	Both probes on rt. ankle
28	28.6	26.6	38.2	Both probes on rt. ankle
29	27.7	31.9	47.1	Both probes on left ankle
30	28.9	31.9	51.0	Both probes on left ankle
33	47.9	40.4	39.8	Both probes on left ankle
34	46.8	40.4	41.2	Both probes on left ankle
35	47.3	29.8	32.2	Both probes on left ankle
36	47.3	30.3	32.7	Both probes on left ankle

The human volunteer had his right leg raised, and both arms at the sides, for tests 29-30. He was 32 m from the center of the simulator and faced this center. Both current probes were on the left ankle. The mean field strength for these 2 tests is 28.3 kV/m, and the mean values of peak current are 31.9 A with the non-ferrous probe and 49.0 A with the Eaton probe. These currents are somewhat greater than those with both legs down, because when the right leg is raised the total current must pass to ground through the left leg, where the current was measured.

In the last series, tests 33-36, the human volunteer was 21 m from the center of the simulator, where the field strength was about 50 kV/m, which is the maximum approved for this project. The subject stood, with arms at the sides, facing the center of the simulator. The subject stood on a 1 m square aluminum plate to increase coupling to ground, and both current probes were on the left ankle. The mean field strength for these 4 tests is 47.3 kV/m, and the mean values of peak current are 35.2 A with the non-ferrous probe and 36.5 A with the Eaton probe.

Currents measured at the EMPRESS I facility are roughly 30 % of those which were measured at ALECS. One reason for part of this difference is that we used peak current, rather than the extreme peak-to-peak currents used for ALECS. Also, there is a metal ground plane at ALECS, which is why the 1 m square aluminum plate was used in the last series of tests. A detailed analysis of the data, including Fourier analyses of the incident fields and the currents, and some numerical solutions, would be required for a complete understanding of the data, and that is beyond the scope of the present project.

## 10. SUGGESTIONS FOR FUTURE WORK

In Section 5 of this report it was stated that we have made and tested several current probes with conductive coils, in which the characteristic impedance of the coil/shield transmission line is about 50 ohms. These probes offer the promise of greater bandwidth without resistive loading, but they are still in a developmental stage so probes with resistive windings were furnished by us on the present contract. We plan to continue the development of current probes with conductive coils and hope that this can be funded at a later date.

## 11. REFERENCES

1. Hagmann, M. J., and T. M. Babij. Device for Non-Perturbing Measurement of Current as a Dosimeter for Hyperthermia, p. 51. Abstracts of Papers for the 8th Annual Meeting of the North American Hyperthermia Group, Philadelphia, PA, 1988.
2. Hagmann, M. J., and T. M. Babij. High Frequency Ammeter, U. S. Patent Number 4,897,600, issued January 30, 1990.
3. Hagmann, M. J., and T. M. Babij. Personal Dosimeter, U. S. Patent Number 4,913,153, issued April 3, 1990.
4. Babij, T. M., and M. J. Hagmann. Noninvasive Measurement of RF Current for Dosimetry, p. 65. The Bioelectromagnetics Society 10th Annual Meeting Abstracts, Stamford, CN, 1988.
5. Miller, E. K. Time-Domain Measurements in Electromagnetics, pp. 283-286. New York: Van Nostrand Reinhold Company Inc., 1986.
6. Ricketts, L. W., J. E. Bridges, and J. Miletta. EMP Radiation and Protective Techniques, p. 231. New York: John Wiley, 1976.
7. Gronhaug, K-L. Antenna Effect of the Human Body to EMP, FFI/NOTAT-83/4042, Norwegian Defence Research Establishment, 1983.
8. Gronhaug, K-L. Measurements and Calculations of Current Induced in a Human Body by EMP Illumination, FFI/NOTAT-86/4008, Norwegian Defence Research Establishment, 1986.
9. Gronhaug, K-L. Measurements of EMP Induced Currents in the Human Body, FFI/NOTAT-88/4038, Norwegian Defence Research Establishment, 1988.
10. Allen, S. G., R. P. Blackwell, and C. Unsworth. Fields and Induced Body Currents in the Vicinity of 2-50 MHz Monopole Anten-



nas, p. 55. The Bioelectromagnetics Society 10th Annual Meeting Abstracts, Stamford, CN, 1988.

11. Guy, A. W. Analysis of Time Domain Induced Current and Total Absorbed Energy in Humans Exposed to EMP Electric Fields, Final Report, Prepared for ERC Facilities Service Corporation, Fairfax, VA, 1989.

12. Hagmann, M. J., and O. P. Gandhi. Numerical Calculation of Electromagnetic Energy Deposition in Models of Man with Grounding and Reflector Effects, Radio Science, Vol. 14, pp. 23-29. November-December, 1979.

13. Kraus, J. D. Electromagnetics, pp. 388-395. New York: McGraw-Hill Book Company, 3rd ed., 1984.